Nuclear Engineering and Design 246 (2012) 2–11

Contents lists available at ScienceDirect

Nuclear Engineering and Design

journal homepage: www.elsevier.com/locate/nucengdes

Appropriate thermodynamic cycles to be used in future pressure-channel supercritical water-cooled nuclear power plants

Laure Lizon-A-Lugrin [a], Alberto Teyssedou [a,*], Igor Pioro [b]

[a] Nuclear Engineering Institute, Engineering Physics Department, École Polytechnique de Montréal, Montréal, Québec, Canada
[b] Faculty of Energy Systems and Nuclear Science, University of Ontario Institute of Technology, Oshawa, Ontario, Canada

ARTICLE INFO

Article history:
Received 8 April 2011
Received in revised form 13 July 2011
Accepted 16 July 2011

ABSTRACT

As member of the Generation IV International Forum (GIF), Canada has decided to orient its efforts towards the design of a CANDU-type SuperCritical Water-cooled nuclear Reactor (SCWR). Such a system must run at a coolant outlet temperature of about 625 °C and at a pressure of 25 MPa. Even though several steam-cycle arrangements used in existing thermal-power plants have been discussed by many authors, none of the proposed cycles have been optimized and adapted to the pressure-channel SCWR concept. The present work is intended to fulfil this gap by including at least two alternative solutions of SCWR power cycles that could reheat the supercritical water in the reactor core to achieve a net mechanical power of 1200-MW. Thus, thermodynamic models for preselected power cycles, their validation among existing data as well as their optimization using an "evolutionary optimization" technique based on genetic algorithms are presented and discussed.

1. Introduction

The International Atomic Energy Agency (IAEA) has recently stipulated that by the year 2030 world primary-energy requirements will increase by up to 45%. To assure both a healthy world economy and adequate social standards, in a relatively short term, new energy-conversion technologies are mandatory. It is obvious that present observed trends in energy supply and consumption do not satisfy environmental sustainability. To fulfil this requirement, the participation of 10 countries has recently made it possible to establish a Generation IV International Forum (GIF). Within this framework, GIF members' have proposed the development of new generation of nuclear-power reactors to replace present technologies. The principal goals of these nuclear-power reactors, among others are: economic competitiveness, sustainability, safety, reliability and resistance to proliferation. Besides the high efficiency that should characterize such a system, it must also permit other energy applications, i.e., hydrogen production, seawater desalinisation or petroleum extraction, to be achieved.

In addition, from a heat-transfer viewpoint, the use of a supercritical fluid allows the limitation imposed by Critical Heat Flux (CHF) conditions, which characterize actual technologies, to be avoided. Furthermore, it will be also possible to use direct thermodynamic cycles where the supercritical fluid expands right away in a turbine without the necessity of using intermediate steam generators and/or separators. Encouraged by these facts, the conventional power industry has implemented supercritical water boiler in the 50s and 60s (Leyzerovich, 2008). These fossil-fuelled units reached thermal efficiencies higher than 40% with supercritical water at about 25 MPa and 600 °C.

The idea of extending the use of superficial water to nuclear power reactors, however, is not new, the first studies in this area were carried out in the 1960s (Aase et al., 1963; Keyfitz et al., 1964). Thus, pressure-vessel Supercritical Cooled Water Reactors (SCWRs) have been largely studied in Japan since 1989. Recently, an international joint collaboration has made it possible the development of a supercritical-water fast neutron reactor concept (Mori, 2005; Yoo et al., 2007; Nakatuska et al., 2010). Even though the reactor pressure vessel resemble the layout of actual pressurized light water reactor's, for the same thermal power it requires much less water inventory (i.e., around pseudo critical conditions the specific heat increases quite rapidly). In addition the use of fast neutrons avoids using a moderator which also contributes in reducing the amount of fluid in the reactor core. Besides these potential technologies, the Canadian nuclear industry is involved to develop a SCWR similar to actual CANDU systems that will run at a coolant outlet temperature of about 625 °C and at pressure of 25 MPa (Duffey et al., 2008; Pioro and Duffey, 2007). It is important to remark that the use of pressure tubes instead of a pressure vessel, in principle should permit the use of advanced steam-reheat thermodynamic cycles. It is obvious that at such conditions the overall efficiency of this kind of Nuclear Power Plant (NPP) will largely compete with actual supercritical water-power boilers. However, future development of NPPs still

* Corresponding author.
E-mail addresses: laure.lizon-a-lugrin@polymtl.ca (L. Lizon-A-Lugrin), alberto.teyssedou@polymtl.ca (A. Teyssedou), Igor.Pioro@uoit.ca (I. Pioro).

0029-5493/$ – see front matter © 2011 Elsevier B.V. All rights reserved.
doi:10.1016/j.nucengdes.2011.07.024

requires a great amount of work that must be carried out to establish the most reliable and optimal thermodynamic-cycle topology that should be appropriate to future pressure-channel SCWRs.

Similarly to the conventional power industry, reheating the working fluid in a nuclear reactor core also constitutes an excellent way for increasing the thermodynamic performance of nuclear power plants. Even though this is a common process in fossil fuelled power plants, from a neutronic view point it represents major scientific and technological challenges. However, this technology which implies complex design of reactor cores is not new; it has its germs in Russia in the earliest 1950s (Saltanov et al., 2010). Based on these previous works, the Canadian industry has considered that the pressure-channel-type of nuclear reactor seems to be the most suitable design. In fact, the use of independent flow channels should make it possible to implement multiple coolant passages across the reactor core. Thus, they can be subdivided at least in two different groups of fuel channels; one for heating the water up to supercritical conditions and a second group where a coolant reheat can take place. In 1964 a first 100-MW_e nuclear reactor that used steam-reheat was constructed in Russia; a second unit of 200-MW_e followed up in 1967 (Saltanov et al., 2010). The gross thermal efficiency of these two nuclear power plants was about 37–38%.

Russian experiences have demonstrated the possibility of using nuclear-core reheat cycles for industrial application. It is apparent, however, that too much work is still necessary to adapt some of these concepts for designing and implementing reheat-SuperCritical Water-cooled Reactor Nuclear Power Plants (SCWR NPPs). To this end, this paper presents two possible cycle configurations for 1200-MW SCWR NPPs. It must be pointed out that this power capacity corresponds to a conceptual pressure-channel SCWR plant design along with the Canadian nuclear industry has been working during the last few years (Naidin et al., 2009; Lizon et al., 2010). Therefore, in this paper two cycle configurations are developed based on a Russian 660-MW fossil-fuelled power plant project that is intended to run under supercritical water conditions (Kruglikov et al., 2009). It will be constructed near the Tom'-Usinsk site, which already have nine coal-power units with a total capacity of 1272-MW. The commissioning of this power plant is expected to take place somewhere along 2011–2012.

2. Power plant simulation and optimization method

To improve the efficiency of nuclear power plants, similarly to conventional systems, the industry uses steam extractions (i.e., heat regeneration thermodynamics cycle). It is obvious that the problem that must be tackled in this kind of process consists of determining the optimal fractions of steam to be extracted at different turbine stages that will permit operation conditions that correspond to the best compromise between the overall cycle efficiency and the mechanical power produced by the plant to be achieved (Sacco et al., 2002). In fact, while efficiency increases with increasing the number of steam extractions, the net mechanical power decreases with increasing this number. Therefore, combining reheat and regeneration in optimal way, to improve simultaneously the output power and the overall plant efficiency, constitutes a complex multi-objective optimization problem that requires convenient modelling tools (Dipama et al., 2010). Since, plant efficiency and mechanical power are in competition, they cannot be satisfied by a unique choice of decision variables. Therefore, a trade-off between the objective functions that represent these two quantities must be determined. To this aim, in this paper an efficient and robust evolutionary algorithm based on the use of genetic algorithms (Goldberg, 1989; Dipama, 2010) is developed and used. This tool is able to determine non dominated "optimal" solutions that conforms a Pareto's front (Pareto, 1896). This optimization technique is coupled to appropriate power plant thermodynamic simulation models written in Matlab (version R2009b). The plant simulator uses the X-Steam library (Holmgren, 2006) based on IAPWS-97 correlations and it communicates with the optimizer via a "Dynamic Data Exchange"[1] protocol (Fig. 1). The optimizer generates an initial random population of solutions that are then used by a power plant simulation to evaluate thermodynamic states that are invoked to calculate objective functions and constraints required to run, once again, the optimizer. Based on the fitness of the solutions, the best ones are selected to pass crossover and mutation operators (Goldberg, 1989) to reproduce a new population of solutions that should be more efficient than the initial one. This new set seeds the simulator and the process continues until a convenient stop criterion is reached (Dipama et al., 2010; Dipama, 2010).

The metric used to control genetic operators (i.e., probabilities of mutations and crossovers) as well as the strategy used to determine Pareto's optimal solutions based on a non-domination sorting procedure are described in Dipama (2010).

2.1. Plant simulator and thermodynamic modelling

In this paper a reengineering process to adapt a projected supercritical water fossil fuelled plant given in Kruglikov et al. (2009) to a 1200-MW SCWR NPP is proposed. The schematic representation of the original system is shown in Fig. 2. It consists of three turbines running in tandem within a supercritical water reheat-thermodynamic cycle. Supercritical water conditions are: 600 °C and 30 MPa and the expected plant thermal efficiency is close to 51%. It is interesting to note that the high pressure circulation pump (CP in the figure) is driven by a small steam turbine. Furthermore, the system is able to regenerate waste heat from gas streams through two gas cooling heat exchangers (GCHP and GCLP in the figure).

Before adapting this cycle to a SCWR NPP, the power plant shown in Fig. 2 is simulated and optimised using the method presented in Section 2. To this purpose, the X-Steam library is first validated by comparing predicted thermodynamic values with those given in the steam-table of Schmidt (1982). Relative differences, defined with respect to the values of this table are partially compared in Fig. 3. In general, it is observed that the X-Steam library implemented in Matlab systematically underestimate (slightly) both enthalpies and entropies, however, maximum differences of about 1% only occur within the pseudo-critical region characterized by temperatures ranging from 375 to 385 °C. In this particular zone, the specific heat of the fluid reaches its maximum value (Pioro and Duffey, 2007); therefore, the accurate calculation of fluid properties becomes more cumbersome (Kretzschmar and Wagner, 2008). However, for temperatures higher than 400 °C, the errors are consistently lower than 0.2%; note that to avoid data congestion, they are not shown in the figure. In addition, the proposed methodology is also validated by comparing the results of overall plant simulations with available data (Kruglikov et al., 2009). Even though the supercritical fossil fuelled plant shown in Fig. 2 is considered as a reference case, to fulfil the objective of this work (i.e., a SCWR NPP of 1200-MW) it must be slightly modified.

Furthermore, to satisfy the stipulated power, two different nuclear plant configurations are proposed where the SCW boiler in Fig. 2 is replaced by two-pass coolant SCW nuclear reactor cores with outlet fluid conditions of 625 °C and 25 MPa. The first configuration uses two identical units of 600-MW each, while the second one corresponds to a plant similar to Fig. 2, where the mass flow rate distributions along the cycle have been consequently increased. The

[1] Trademark of Microsoft Co.

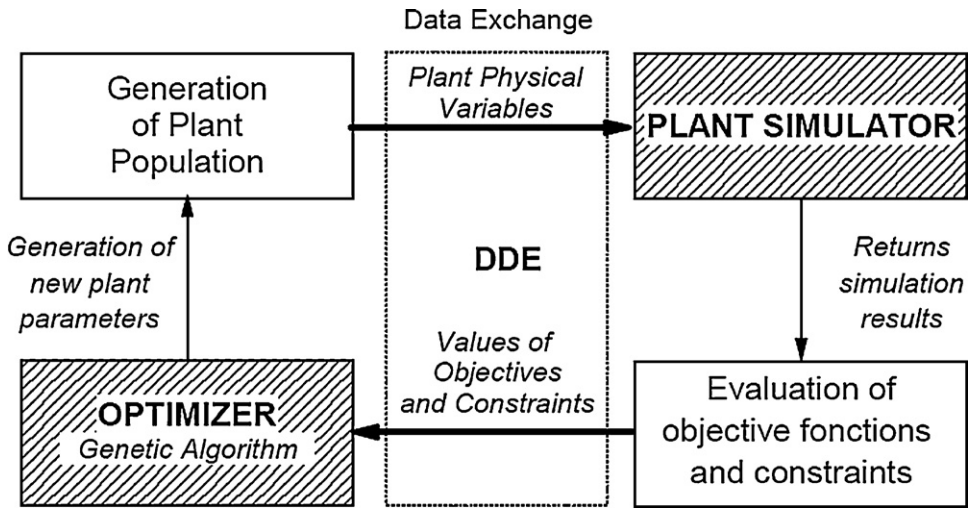

Fig. 1. Plant optimization-simulation procedure.

power plant simulator includes specific models of different thermal equipments that are described in next paragraphs.

Each turbine shown in Fig. 2 is divided into multistage groups according to steam extraction points as presented in Fig. 4. In the plant model, each group is characterized by an isentropic efficiency expressed as:

$$\eta_s = \frac{h_i - h_{i+1}}{h_i - h_{s,\,i+1}} \tag{1}$$

where $h_{s,i+1}$ represents the isentropic specific enthalpy calculated using values given in Duffey et al. (2008). Thus, the mechanical power produced by the turbine is calculated as:

$$|\dot{W}_T| = \dot{m}\left[(h_0 - h_1) + \sum_{i=1}^{n-1}\left(1 - \sum_{k=1}^{i} y_k\right)(h_i - h_{i+1})\right] \tag{2}$$

with $\dot{m}$ the total steam mass flow rate and y_k the extracted fraction of the total flow at stage k in the turbine.

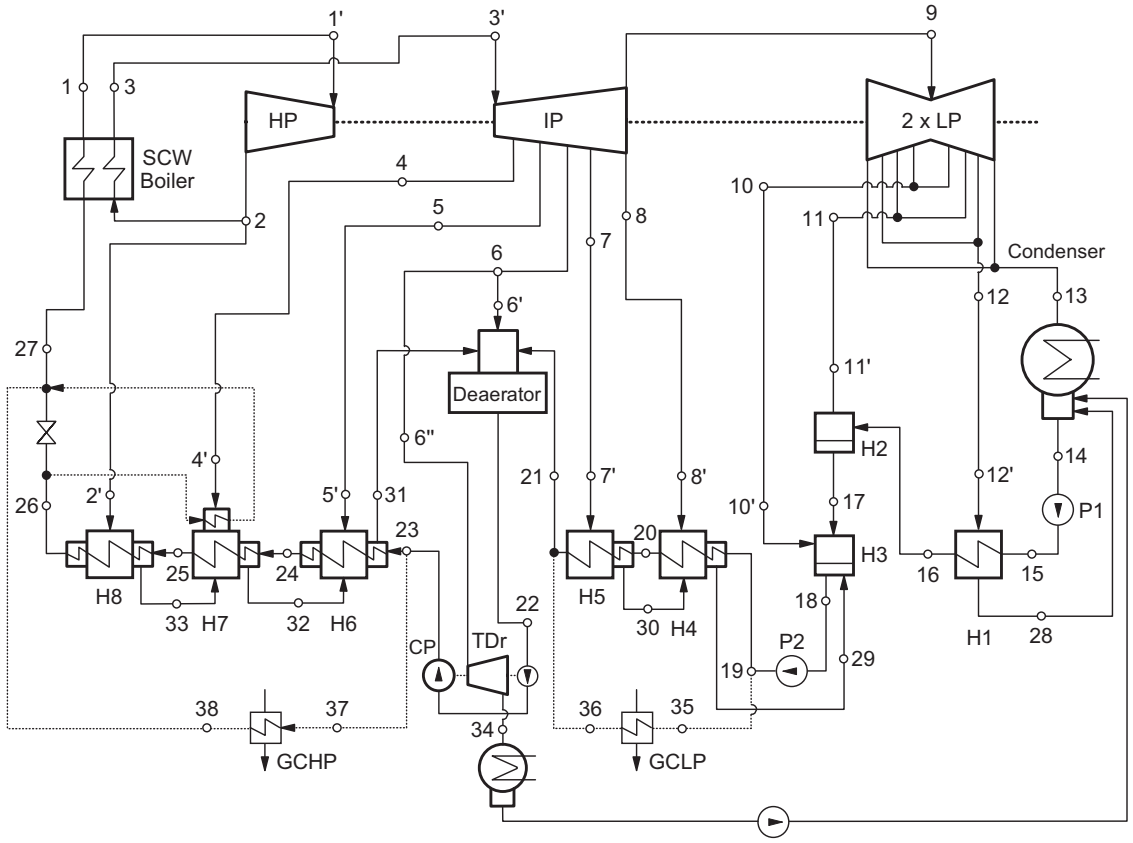

Fig. 2. 669-MW$_e$ Tom'-Usinsk Russian supercritical water fossil fuelled plant (Kruglikov et al., 2009).

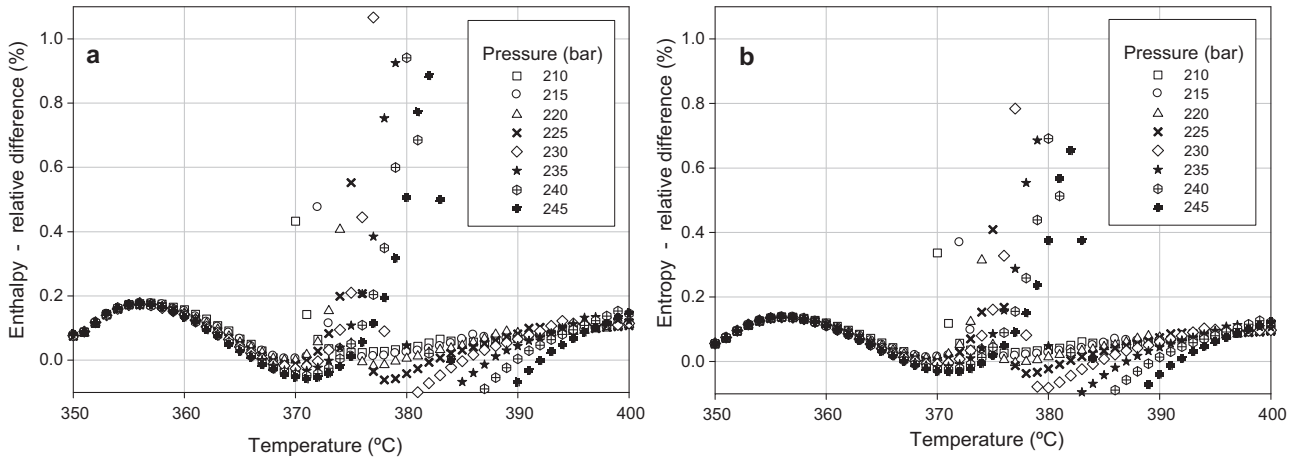

Fig. 3. Comparison of water-steam properties predicted by X-Steam (Holmgren, 2006) with values given in Schmidt (1982): (a) relative enthalpy difference; (b) relative entropy difference.

Feedwater heaters permit the plant thermal efficiency to be increased by regenerating the latent heat of extracted steam fractions. The model used for closed feedwater heaters is based on temperature differences between the extracted steam and the feedwater (Teyssedou et al., 2010). The Terminal Temperature Differences (TTD) and Drain-Cooler Approach (DCA) used in the simulations are calculated from actual plant operation conditions given in Duffey et al. (2008). The scheme of the three-zone feedwater heater is shown in Fig. 5. Instead, for open feedwater heaters, it is assumed that at the outlet the water reaches saturated liquid state. For the deaerator (Fig. 2), saturation conditions which allow non-condensable gases to be extracted are assumed. Further, all simulations are performed for a constant condenser pressure of 3 kPa and by assuming that the condensate exits this unit as saturated liquid.

The model of condensate pumps (P1 and P2 in Fig. 2) is performed by using the specific volume of the fluid determined at the inlet side; these pumps are considered to be ideally isentropic. In turn, the model of the high capacity circulation pump (CP in Fig. 2) takes into account the isentropic efficiency, which was determined as 78.8% by the following expression:

$$\eta_s = \frac{h_i - h_{s,i+1}}{h_i - h_{i+1}} \tag{3}$$

The reference system given in Kruglikov et al. (2009) also provides information about pressure losses along the steam extraction lines. Notice that the thermodynamic states which are affected by these losses are indicated with primes in Fig. 2. To take them into account, the simulation model must use appropriate relationships

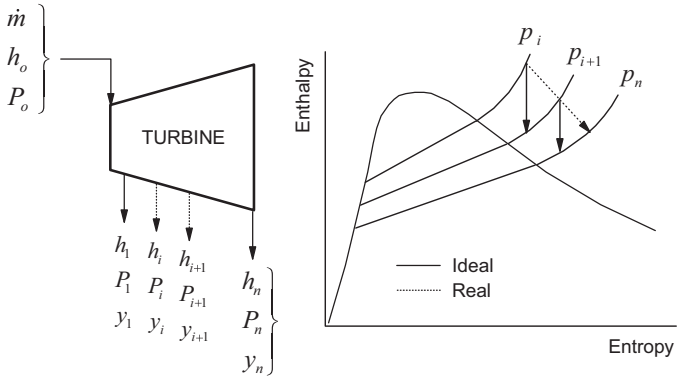

Fig. 4. Simple modelling of multistage turbine groups.

as function of the mass flow rate. Thus, in this work the following proportionality is considered as suitable:

$$\Delta P \, \alpha \, \dot{m}^2 \tag{4}$$

then a pressure loss coefficient for each line is estimated as follows:

$$coef_{\Delta P} = \frac{\Delta P_{reference}}{\dot{m}^2_{reference}} \tag{5}$$

It is assumed that this coefficient characterizes each pipe (i.e., diameter and wall roughness fraction); therefore, the pressure drop caused by different flow rates than those given in the reference case are estimated as:

$$\Delta P_{new} = \dot{m}^2_{new} \times coef_{\Delta P} \tag{6}$$

For the second 1200-MW SCWR NPP configuration, a single cycle based on the scheme shown in Fig. 2, is proposed with a total mass flow rate increased by a factor $k > 1$. However, to maintain pressure drops as close as possible to the reference values (Kruglikov et al., 2009), the $coef_{\Delta P}$ is divided by k^2.

3. Simulation and validation procedures

For validation purposes, the original power plant given in Kruglikov et al. (2009) is first simulated and optimized by using the aforementioned methodology. Table 1 summarizes the reference thermodynamic states as function of the corresponding numbers shown in Fig. 2. The simulation is performed by assuming a deaerator absolute pressure of 1.01 MPa and an absolute condenser pressure of 0.003 MPa. Further, outlet fluids from the deaerator, the condenser and open feedwater heaters are assumed to be under saturation liquid conditions. All other states are determined by mass and energy balances, or by using the relation between isentropic efficiencies and enthalpies (i.e., in turbines and circulation pumps).

The models used for the condenser and feedwater heaters, however, require conserving simultaneously both energy and mass; therefore, an iterative calculation is implemented (Teyssedou et al., 2010). Since the overall model also includes the pressure drop along lines and they may affect local thermodynamic states, an external iteration of the whole system of equation is also used. In all the cases a single convergence criterion of 10^{-6} is applied. Fig. 6 shows a flowchart of the calculation procedures, including a simplified scheme of the optimiser module. Additional information about the optimization as well as genetic operators are given in Dipama (2010) and Teyssedou et al. (2010). During the model

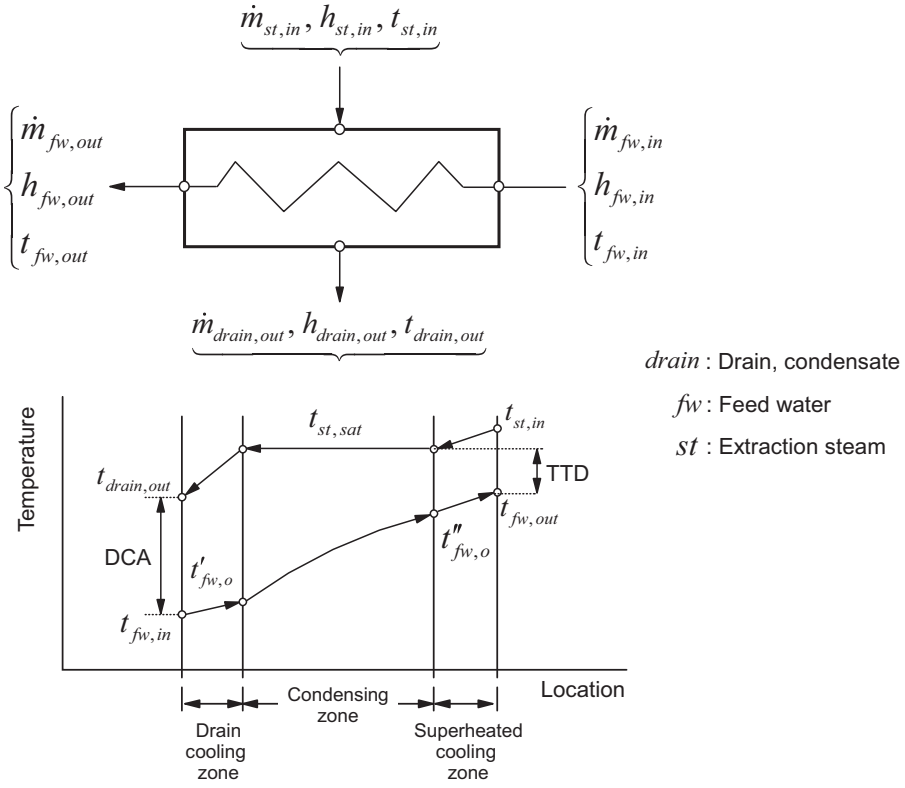

Fig. 5. Flow diagram and temperature profiles of a three-zone feedwater heater.

validation described in this section, however, only the plant simulator is invoked.

The net mechanical power $\dot{W}$ is calculated by subtracting the power consumed by the pumps from that generated by the turbines. The plant thermal efficiency is obtained from the total thermal power input $\dot{Q}_{in}$, hence:

$$\dot{Q}_{in} = \dot{m}(h_1 - h_{28}) + \dot{m}_3(h_3 - h_2), \qquad \eta = \frac{\dot{W}}{\dot{Q}_{in}} \tag{7}$$

It must be pointed out, however, that the gas cooler units (GCHP and GCLP) shown in Fig. 2 as well as the reheat line on the top of heat exchanger H7 are not included in the proposed SCW NPP configurations (they are shown by dashed lines in the figure).

The aforementioned modifications, however, have an impact on both mass and energy balances, in particular for the fraction of extracted steam due to the short of energy provided by the GCHP and GCLP systems. To overcome this drawback and for validation purposes, the gas coolers were replaced by an external heat source. Therefore, the enthalpy differences across the corresponding heat exchangers as well as the feedwater mass flow rates are kept constant. Using the reference values shown in Table 1 yields:

$$\begin{aligned} \dot{Q}_{GCLP} &= \dot{m}_{35}(h_{36} - h_{35}) = 9.42\,\text{MW}, \\ \dot{Q}_{GCHP} &= \dot{m}_{37}(h_{38} - h_{37}) = 17.21\,\text{MW} \end{aligned} \tag{8}$$

Similar calculations performed in the reheat section shown on the top of the heat exchanger H7 (Fig. 2) resulted in 11.24 MW. The results of the simulation of the original power plant are shown in the first five columns on the left side of Table 1. In general, the proposed model reproduces quite well the actual operation conditions of the plant. The difference observed at state 16 is mainly due to the assumption made on the saturated liquid condition at the outlet of the heat exchanger. Indeed, the enthalpy given in the reference is higher than the value of the enthalpy at saturation for the pressure given for this thermodynamic state. Other states shown in boldface in Table 1 correspond to those used for replacing the gas cooling units (GCHP and GCLP). These states are not used for the simulation-optimization to be performed on the proposed SCWR NPPs.

Table 1 shows that the highest difference among calculated mass flow rates is less than 1%. In turn, for temperatures and enthalpies the highest difference is lower than 0.4%. Moreover, both the thermal efficiency and the mechanical power are reproduced with much higher accuracy. These results confirm the good performance of the plant simulator; thus, it can now be used for optimization purposes.

4. Results of plant optimizations

Once the plant modelling method is validated against available power plant data (i.e., without optimization), it is used to perform the optimization of the reference case (Kruglikov et al., 2009) as well as the proposed SCWR NPP configurations. It is apparent that a multi-objective optimization procedure must handle a large number of decision variables and constraints. In this work, pressures at different locations along the power cycle are considered as decision variables. Constraints are imposed based on temperature differences to satisfy the second law of thermodynamics. For all the cases studied, the most important values of decision variables and constraints are summarized in Table 2. The same temperature constraints used for running the reference case are also used to treat the other ones, while the qualities x_{14}, x_{17}, x_{18} and x_{22} are forced to zero. Furthermore, for all cases treated, the mass flow rate at state 12 in Fig. 2 is used as an additional decision variable. Note that the functions given in Eq. (7) are the two objectives that are simultaneously satisfied by fulfilling the aforementioned physical constrains. It is obvious that to satisfy the optimum values of the pressures, the optimizer forces the associated mass flow rates to change. This is

Table 1
Reference and simulated values of the fossil fuelled power plant given in Kruglikov et al. (2009).

State #	Reference values					Simulated values				
	$\dot{m}$ (kg/s)	T (°C)	P (MPa)	h (kJ/kg)	y (%)	$\dot{m}$ (kg/s)	T (°C)	P (MPa)	h (kJ/kg)	y (%)
1	475.9	600.0	30	3447.0		475.89	600.00	30.0	3446.87	
1′	475.9	597.0	29	3447.0		475.89	597.00	29.0	3446.87	
2	475.9	375.4	7.5	3079.4		475.89	375.20	7.5	3079.48	
2′	38.8	372.9	7.2	3079.4		38.70	372.83	7.2	3079.48	
3	437.1	620.0	7.3	3695.7		437.20	620.00	7.3	3695.84	
3′	437.1	619.7	7.2	3695.7		437.20	619.67	7.2	3695.84	
4	20.8	541.1	4.6	3534.5		20.80	541.30	4.6	3534.51	
4′	20.8	540.3	4.4	3534.5		20.80	540.47	4.4	3534.51	
5	29.1	457.9	2.7	3366.2		29.10	457.80	2.7	3366.21	
5′	29.1	457.2	2.6	3366.2		29.10	457.25	2.6	3366.21	
6	51.1	330.2	1.1	3113.7		51.10	330.10	1.1	3113.71	
6′	19.6	329.3	1	3113.7		19.60	329.07	1	3113.71	
6″	31.5	328.8	0.97	3113.7		31.50	328.76	0.97	3113.71	
7	9.1	235.3	0.5	2930.3		9.10	235.20	0.5	2930.32	
7′	9.1	234.7	0.471	2930.3		9.10	234.68	0.471	2930.32	
8	18.2	191.9	0.333	2847.4		18.30	191.80	0.333	2847.42	
8′	18.2	191.3	0.314	2847.4		18.30	191.36	0.314	2847.42	
9	308.8	191.6	0.32	2847.4		308.70	191.50	0.32	2847.42	
10	13.4	NA	0.104	2655.7	0.93	13.50	100.70	0.104	2655.71	0.93
10′	13.4	NA	0.097	2655.7	0.79	13.50	98.74	0.097	2655.71	0.79
11	13.6	NA	0.043	2530.9	4.68	13.50	77.60	0.043	2530.90	4.67
11′	13.6	NA	0.04	2530.9	4.56	13.50	75.88	0.04	2530.90	4.54
12	17.3	NA	0.018	2422.9	7.67	17.30	57.80	0.018	2422.90	7.71
12′	17.3	NA	0.0167	2422.9	7.55	17.30	56.21	0.0167	2422.90	7.58
13	264.4	NA	0.003	2267.6	11.35	264.40	24.10	0.003	2267.60	11.35
14	313.2	24.1	0.003	100.9		313.30	24.10	0.003	100.99	
15	313.2	24.1	0.49	101.7		313.30	24.10	0.49	101.48	
16	**313.2**	**53.0**	**0.39**	**222.3**		**313.30**	**52.90**	**0.39**	**221.94**	
17	326.9	76.1	0.04	318.6		326.80	75.90	0.04	317.66	
18	367.6	98.8	0.097	414.1		367.80	98.70	0.097	413.77	
19	367.6	99.0	1.37	415.7		367.80	98.80	1.37	415.09	
20	321.8	131.9	1.27	555.2		321.90	131.90	1.27	555.01	
21	367.6	147.4	1.18	621.3		367.80	147.40	1.18	621.36	
22	475.9	180.3	1.01	764.5		475.90	180.34	1.01	764.59	
23	475.9	187.1	34.3	811.8		475.90	187.20	34.3	811.90	
24	440.8	231.6	34	1006.1		440.80	231.60	34.0	1006.32	
25	440.8	NA	33.7	1107.4		440.80	254.10	33.7	1107.68	
26	440.8	289.8	33.3	1277		440.80	289.80	33.3	1276.61	
27	**475.9**	**295.0**	**33.2**	**1302.5**		**475.90**	**294.90**	**33.2**	**1302.15**	
28	17.3	56.0	0.017	234.5		17.30	56.22	0.017	235.31	
29	27.4	109.0	0.31	457.2		27.40	108.80	0.31	456.51	
30	9.1	141.9	0.47	597.5		9.10	141.90	0.47	597.26	
31	88.7	197.1	2.6	839.9		88.60	197.20	2.6	840.25	
32	59.6	241.6	4.4	1045.4		59.50	241.60	4.4	1045.50	
33	38.8	264.0	7.2	1154.3		38.70	264.10	7.2	1154.64	
34	31.5	NA	0.006	2405.3		31.50	36.20	0.006	2405.27	
35	**45.8**	**99.0**	**1.37**	**415.7**		**45.80**	**98.82**	**1.37**	**415.09**	
36	**45.8**	**147.4**	**1.18**	**621.3**		**45.80**	**147.41**	**1.18**	**621.45**	
37	**35.1**	**187.1**	**34.3**	**811.8**		**35.10**	**187.20**	**34.3**	**811.90**	
38	**35.1**	**295.0**	**33.2**	**1302.5**		**35.10**	**294.93**	**33.2**	**1302.11**	

NA: not available.

Table 2
Optimization decision variables and constraints.

Decision variables: pressure (MPa)		
Reference case 668-MW fossil fuelled supercritical power plant (Kruglikov et al., 2009)	Proposed SCWR NNPs 600-MW and 1200-MW	Temperature constraints (°C) all system
$6.6 \le P_2 \le 9.0$	$5.0 \le P_2 \le 6.5$	$tsat_{H8} - t_{33} > 0$
$3.6 \le P_4 \le 6.5$	$3.5 \le P_4 \le 4.8$	$tsat_{H7} - t_{32} > 0$
$1.5 \le P_5 \le 3.5$	$1.2 \le P_5 \le 3.4$	$tsat_{H6} - t_{31} > 0$
$0.4 \le P_7 \le 0.8$	$0.4 \le P_7 \le 0.8$	$tsat_{H5} - t_{30} > 0$
$0.2 \le P_8 \le 0.4$	$0.2 \le P_8 \le 0.4$	$tsat_{H4} - t_{29} > 0$
$0.07 \le P_{10} \le 0.20$	$0.07 \le P_{10} \le 0.20$	
$0.03 \le P_{11} \le 0.06$	$0.03 \le P_{11} \le 0.06$	
$0.015 \le P_{12} \le 0.02$	$0.015 \le P_{12} \le 0.020$	

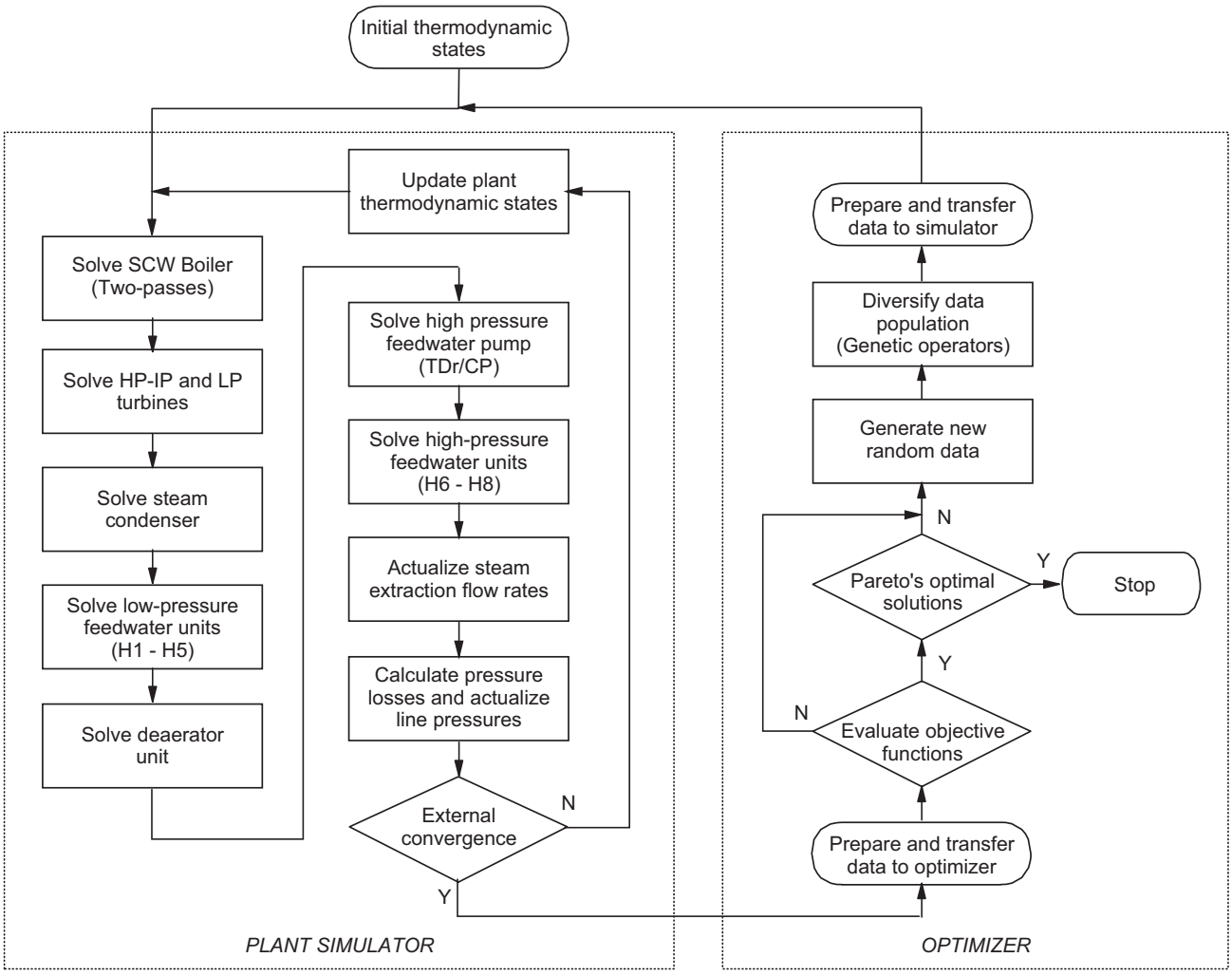

Fig. 6. Simplified flowchart of calculation procedures, including the optimization module.

an important point that should be considered in future reengineering work. In fact, adjusting extraction flow rates to their optimal values could necessitate the redimension of some steam lines to satisfy maximum pressure loss requirements.

The Pareto's front obtained for the reference case is shown in Fig. 7. It is interesting to observe that the actual operation conditions of this fossil fuelled power plant are quite close to Pareto's boundary (i.e., $\dot{W} = 668.7$ MW and $\eta = 50.8\%$), i.e., the difference with respect to the front is less than 1 point of percentage. These results clearly show that the project described in Kruglikov et al. (2009) seems to have been already optimized and well designed to obtain an almost optimal value of thermal efficiency. However, from Fig. 7, it is obvious that the present optimization method provides a wider range of conditions under which the plant could perform better by decreasing the net mechanical power or vice versa (i.e., two competing objectives). The final selection of best trade-offs must follow not only economical conditions (reduce fuel expenditures with decreasing the net available power) but technical criteria that were used for designing the plant (i.e., turbines, heat exchangers, and condenser).

For the SCWR NPP cases, temperatures, pressures and mass flow rates are different than the reference case. In particular, pressures and temperatures are modified to satisfy the anticipated operation conditions of future SCWRs (Duffey et al., 2008; Naidin et al., 2009; Lizon et al., 2010). Thus, the pressure in the reactor core is fixed to 25 MPa and the outlet fluid temperature to 625 °C. During the reheat process, however, the pressure during the second passage of the fluid in the reactor core is much lower than 6.5 MPa.

The Pareto's front obtained for the proposed SCWR NPP configurations as well the values obtained from the simulations before the optimization is performed, are shown in Fig. 8a and b. For two

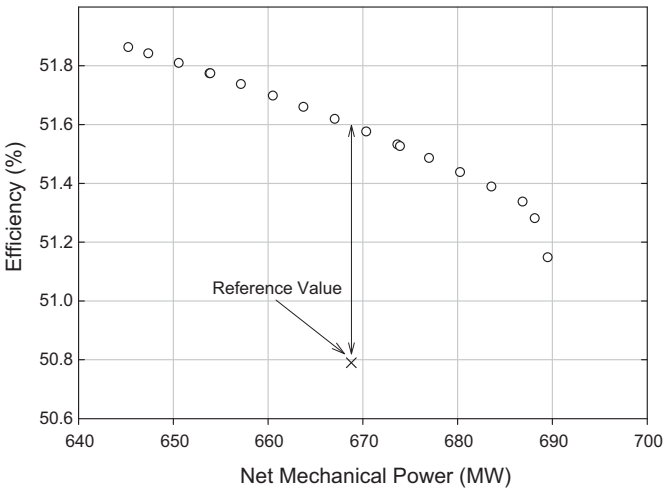

Fig. 7. Pareto's front obtained for the reference case (Kruglikov et al., 2009).

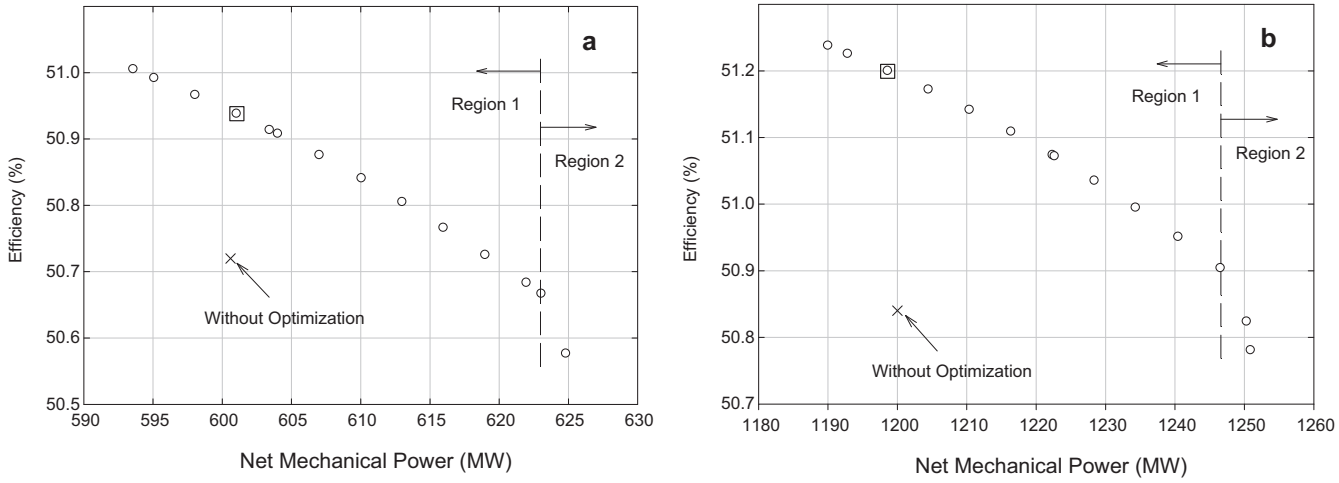

Fig. 8. Pareto's front for SCWR NPP's: (a) 600-MW units; (b) single 1200-MW unit.

600-MW SWCR units running in parallel (Fig. 8a) a steam mass flow rate by loop of 412 kg/s is used; for the 1200-MW system (Fig. 8b) this value is doubled.

It is apparent that for a net mechanical power equal to the non-optimized one, the optimization permits increasing the efficiency by about 0.2 and 0.35 points of percentage, respectively. Once again, it is observed that both the optimum values of efficiency and net power vary in opposite directions. The results of these cycle simulations and optimizations for a net power close to the stipulated values (points signposted on the Pareto's front in Fig. 8) are given in Table 3. For both optimizations the results are very close, indeed the thermal efficiency is higher by about 0.2 points of percentage for the single 1200-MW unit. It may be explained by the higher temperature at the inlet of reheat process at state 2. On the other hand, the real net mechanical power produced by the 2×600-MW units is higher by about 4 MW. Thus the optimization reaches almost the same global behaviour for both cycles. Broadly, values of pressures at the extractions, which are the decision variables in the optimization process, are quite similar. Whereas, the mass flow rate at the extraction of state 12 which is a decision variable, is 2.6 times higher than the value for 2×600-MW units. This fact has an impact on the value of the temperature for states 16–21, and can probably affect the thermal efficiency of the thermodynamic cycle.

It must be pointed out that there is not a single solution to any non-deterministic optimization problem. Instead there are a set of solutions that randomly converge towards a Pareto's front (Dipama, 2010). Therefore, a decision maker is necessary in order to determine the appropriate selection of the solutions that integrate the front. It is obvious that the selection of solutions depends on a trade off over the multi-objective solution space. Furthermore, depending on the nature of the problem, the behaviour of different solutions as a function of decision variables can be quite complex. Consistent with this view point, Fig. 8 represents plane projections of a complex multidimensional space (i.e., Pareto's front), which according to their slopes can be divided in two distinct regions. Close analysis of changes observed in the decision variables during the optimization shown in Fig. 8a, have indicated that the first region seems to be mainly controlled by the pressure at state 2 where efficiency increases with increasing the pressure. However, the net mechanical power decreases with increasing the same pressure. It is also observed that the corresponding mass flow rate of extracted steam tends to increase. This change increases feedwater reheating which in turn increases the water enthalpy at the entrance of the reactor core. This behaviour is directly correlated to the thermal efficiency of the cycle. Instead, the second region follows a more complex behaviour that seems to be controlled by pressures at states 4 and 5, and by the mass flow rate of extraction 12 (Fig. 2). Even though other variables also vary during the process, no apparent correlation between them and the Pareto's landscape was able to be established.

For the second SCWR NPP configuration, the change in mass flow rate affects the overall mass balances along the cycle. Fig. 8b shows that the Pareto's front can be also divided into two regions. The behaviour of the several decision variables is quite similar to the previous case (Fig. 8a), i.e., region 1 is mainly controlled by the value of pressure at state 2 as shown in Fig. 9a. Thus, efficiency increases and net mechanical power decreases with increasing the pressure. Increasing the reheat pressure allows a higher average temperature during the heat-addition process which is a common way for increasing the thermal efficiency in a Rankine cycle. For this case, it is also observed that within a very limited range, the efficiency is essentially affected by the extractions at states 2 and 12 (see Fig. 2), while the effects of variations on other mass flow rates are negligible. Fig. 9b shows the variation of the mass flow rate at state 2 which as the previous case reheats the feedwater through the last heat exchanger. In the same way than increasing the pressure, it allows a higher average temperature for heat-addition process and thus has the effect to increase the thermal efficiency of the cycle. The second region seems to be controlled by the pressure at the first steam extraction in the IP turbine while all other decision variables remain almost constant in this region.

In general it is observed that the improvement in the mechanical power can be substantial, while conditions imposed by the deaerator limit considerably the possibility to enhance plant's efficiency. These conditions, however, are necessary to guarantee acceptable removal of non-condensable gases.

From an engineering view point, the first SCWR NPP configuration will necessitate doubling mechanical and nuclear components which will increase both investment and operational cost. In turn, the fact that the second configuration requires much higher mass flow rates, will involve different dimensioning of major thermal components, i.e., turbines, heat exchangers, condenser, and main circuit pumps. Any of these modifications can also affect the internal power requirement of the plant and consequently may have an effect on the overall plant performance. Furthermore, a trade-off between two NPP possibilities will still necessitate a multi-objective optimization that should include appropriate economic models.

Table 3
Simulation-optimization results for the reference case and proposed SCWR NPPs.

State #	Initial values for fossil-fuelled power plant (Kruglikov et al., 2009)			Optimised values for 2 × 600-MW SCWR NPP			Optimised values for 1200-MW SCWR NPP		
	T (°C)	P (MPa)	$\dot{m}$ (kg/s)	T (°C)	P (MPa)	$\dot{m}$ (kg/s)	T (°C)	P (MPa)	$\dot{m}$ (kg/s)
1	600.0	30.0	475.9	625.0	25.00	412.0	625.0	25.0	821.3
2	375.4	7.5	475.9	394.9	6.11	34.0	399.6	6.3	69.2
3	620.0	7.3	437.1	625.0	5.96	378.0	625.0	6.05	752.1
4	541.1	4.6	20.8	534.4	3.50	11.1	532.7	3.50	21.8
5	457.9	2.7	29.1	466.8	2.27	23.2	466.3	2.29	45.7
6	330.2	1.1	51.1	361.3	1.10	51.1	359.8	1.10	51.1
7	235.3	0.5	9.1	236.9	0.40	10.1	235.7	0.40	15.4
8	191.9	0.333	18.2	182.6	0.24	17.5	195.6	0.28	28.0
9	191.6	0.32	308.8	182.2	0.23	264.9	195.3	0.23	590.1
10	100.7	0.104	13.4	89.9	0.07	11.7	110.4	0.10	14.8
11	77.6	0.043	13.6	65.8	0.026	10.0	85.8	0.0597	10.0
12	57.8	0.018	17.9	54.0	0.015	10.6	54.0	0.015	55.5
13	24.1	0.003	264.4	24.1	0.003	232.6	24.1	0.003	509.7
14	24.1	0.003	313.2	24.1	0.003	272.0	24.1	0.003	572.6
16	53.0	0.39	313.2	44.7	0.39	272.0	76.1	0.39	572.6
17	76.1	0.04	326.9	64.4	0.02	282.0	85.6	0.06	582.6
18	98.8	0.097	367.6	87.8	0.06	321.3	100.1	0.10	640.8
19	99.0	1.37	475.9	87.9	1.37	321.3	100.2	1.37	640.8
23	187.1	34.3	475.9	186.0	28.22	412.0	186.2	29.30	821.3
24	231.6	34.0	440.8	223.0	28.00	412.0	223.0	29.00	821.3
25	254.0	33.7	440.8	239.6	27.77	412.0	239.3	28.70	821.3
26	289.8	33.3	440.8	276.2	27.47	412.0	277.0	28.30	821.3
27	295.0	33.2	475.9	276.2	27.47	412.0	277.0	28.30	821.3
η (%)		50.79			50.94			51.20	
$\dot{W}$ (MWe)		668.78			601.06			1198.66	

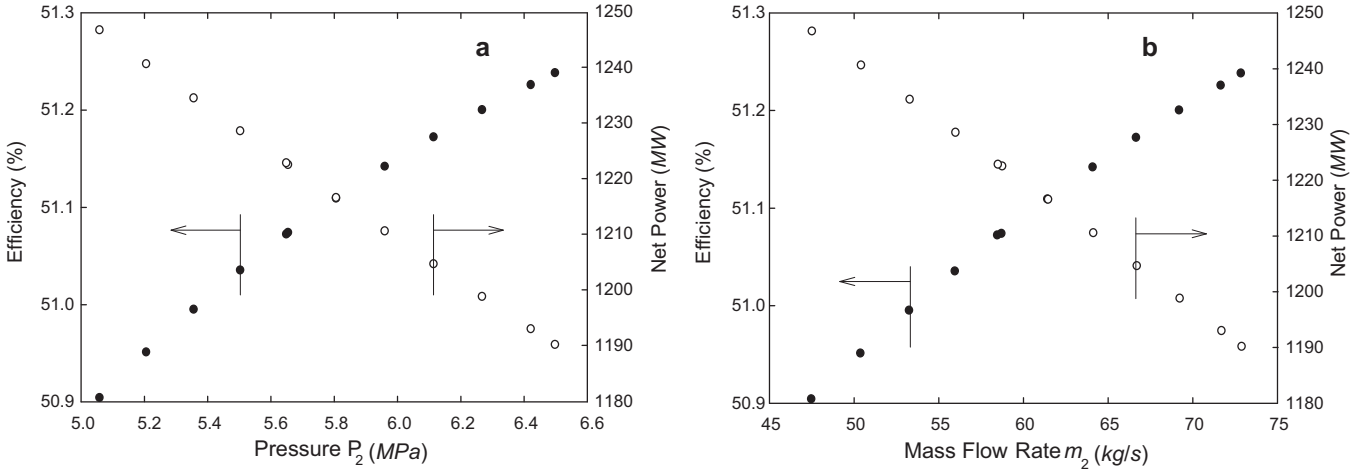

Fig. 9. Variations of efficiency and net power: (a) as a function of pressure P_2; (b) as a function of mass flow rate $\dot{m}_2$.

5. Conclusion

A plant modelling approach coupled to an evolutionary optimization technique is presented. The model is validated by comparing its prediction with data taken from a projected Russian fossil fuelled supercritical water plant. The same model and plant layout are then slightly modified and used to produce suitable topologies for future SCWR NPP based on core coolant–reheat cycles. The first option, which consists of two 600-MW units running in parallel, needs a total water mass flow rate of 412 kg/s per loop. The optimization of such a system shows a Pareto's landscape that offer a quite large spectrum of possible operation conditions. The optimisation of the second SCWR NPP system consisting of a single 1200-MW unit produces a Pareto's front having similar features with a mechanical power ranging from 1190 to 1250-MW. In both cases it is observed that the front can be subdivided in two distinct regions where the optima seem to be controlled only by a limited number of decision variables. This observation may help process engineers in achieving more appropriate power plant designs by starting from actual SCW conventional power plant concepts. In addition, this work clearly shows that even though efficiency and mechanical power are competing objectives, Pareto's fronts indicate that it is still possible to improve simultaneously both of them.

Acknowledgments

This work was funded by the Natural Sciences and Engineering Research Council of Canada discovery grant RGPIN 41929 and the Hydro-Québec Chair in Nuclear Engineering.

References

Aase, D.T., et al., 1963. Economic Evaluation of a 300 MWe Fast Supercritical Pressure Power Reactor. Engineering Development Reactor and Fuels Laboratory, Hanford Laboratories (GE contract HW-78953, Dec. 9).

Dipama, J., 2010. Optimisation multi-objectif des systèmes énergétiques. Thèse de Doctorat. École Polytechnique de Montréal, Avril.

Dipama, J., Teyssedou, A., Aubé, F., Lizon-A-Lugrin, L., 2010. A grid based multi-objective evolutionary algorithm for the optimization of energy systems. App. Therm. Eng. 30, 807–816.

Duffey, R.B., Pioro, I.L., Zhou, T., Zirn, U., Kuran, S., Khartabil, H., Naidin, M., 2008. Supercritical water-cooled nuclear reactors (SCWRs): current and future concepts—steam cycle options. In: Proceedings of the 16th International Conference on Nuclear Engineering, Florida, USA.

Goldberg, D.E., 1989. Genetic Algorithms in Search, Optimization, and Machine Learning. Addison-Wesley, Reading, pp. 412.

Holmgren, M., 2006. X Steam for Matlab, Edition.

Keyfitz, et al., 1964. 1000 MWe Supercritical Pressure Nuclear Power Plant Design Study. Westinghouse Electric Co (Report # WCAP 2240).

Kretzschmar, H.-J., Wagner, W., 2008. International Steam Tables: Properties of Water and Steam Based on the Industrial Formulation IAPWS-IF97, second edition. Springer-Verlag, Berlin.

Kruglikov, P.A., Smolkin, Yu.V., Sokolov, K.V., 2009. Development of Engineering Solutions for Thermal Scheme of Power Unit of Thermal Power Plant with Supercritical Parameters of Steam. In: Workshop on Supercritical Water and Steam in Nuclear Power Engineering: Problems and Solutions, Moscow, Russia (in Russian).

Leyzerovich, S., 2008. Steam Turbines for Modern Fossil-Fuel Power Plants. Fairmont Press, Inc., Lilburn.

Lizon-A-Lugrin, L., Teyssedou, A., Pioro, I., 2010. Optimization of power-cycle arrangements for supercritical water cooled reactors (SCWRS). In: Proceedings of the 31st Annual Conference of the Canadian Nuclear Society, May 24–27, Montreal, Canada.

Mori, M., 2005. Core Design Analysis of the Supercritical Water Fast Reactor. Institut für Kern-und Energietechnik Programm Nukleare Sicherheitsforschung, Karlsruhe (FZKA 7160, October).

Naidin, M., Mokry, S., Baig, F., Gospodinov, Y., Zirn, U., Pioro, I., Naterer, G., 2009. Thermal-design options for pressure-channel SCWRS with cogeneration of hydrogen. Journal of Engineering for Gas Turbines and Power 131, 012901–012908.

Nakatsuka, T., et al., 2010. Current status of research and development of supercritical water-cooled fast reactor (super fast reactor) in Japan. In: IAEA Technical Meeting on SCWRs, July 5–8, Pisa.

Pareto, V., 1896. In: Rouge, F. (Ed.), Cours d'économie politique. , Lausanne.

Pioro, I.L., Duffey, R.B., 2007. Heat Transfer and Hydraulic Resistance at Supercritical Pressures in Power Engineering Applications. ASME Press, New York.

Sacco, W.F., Pereira, C.M.N.A., Soares, P.P.M., Schirru, R., 2002. Genetic algorithms applied to turbine extraction optimization of a pressurized-water reactor. Appl. Energy 73 (3), 217–222.

Saltanov, E., Monichan, R., Tchernyavskaya, E., Pioro, I., 2010. Nuclear steam-reheat options: Russian experience. In: Proceedings of the 2nd Canada-China Workshop SWCR, Canada.

Schmidt, E., 1982. Properties of Water and Steam in SI-Units, third edition. Springer-Verlag, Berlin.

Teyssedou, A., Dipama, J., Hounkonnou, W., Aubé, F., 2010. Modeling and optimization of a nuclear power plant secondary loop. Nucl. Eng. Des. 240, 1403–1416.

Yoo, J., et al., 2007. Subchannel analysis of supercritical light water-cooled fast reactor assembly. Nucl. Eng. Des. 237, 1096–1105.